JOURNAL OF PROPULSION AND POWER
Vol. 15, No. 1, January–February 1999

Flow Coupling Effects in Jet-in-Crossflow Flowfields

D. B. Bain* and C. E. Smith†
CFD Research Corporation, Huntsville, Alabama 35805
D. S. Liscinsky‡
United Technologies Research Center, East Hartford, Connecticut 06108
and
J. D. Holdeman§
NASA Lewis Research Center, Cleveland, Ohio 44135

The combustor designer is typically required to design liner orifices that effectively mix airjets with crossflow effluent. Computational fluid dynamics (CFD) combustor analysis is typically used in the design process; however, the jets are usually assumed to enter the combustor with a uniform velocity and turbulence profile. The jet–mainstream flow coupling is usually neglected because of the computational expense. This study was performed to understand the effect of jet and mainstream flow coupling, and to investigate jet boundary conditions that are commonly used in combustor internal calculations. A case representative of a plenum-fed quick-mix section of a rich burn/quick mix/lean burn combustor, i.e., a jet to mainstream mass-flow ratio of about 3 and a jet to mainstream momentum-flux ratio of about 30, was investigated. This case showed that the jet velocity entering the combustor was very nonuniform, with a low normal velocity at the leading edge of the orifice and a high normal velocity at the trailing edge of the orifice. Three different combustor-only cases were analyzed, each with a uniform inlet jet profile. None of the cases matched the plenum-fed calculations. To assess liner thickness effects, a thin-walled case was also analyzed. The CFD analysis showed the thin-walled jets had more penetration than the thick-walled jets.

Nomenclature

A_i = flow area of cell i
A_j/A_∞ = ratio of jet orifice area to mainstream cross-sectional areas
A_{tot} = total flow area in each axial plane
C_{av} = $m_j/(m_j + m_\infty)$, θ_{EB}
C_i = jet mass fraction in cell I
C_{var} = $(1/A_{tot})\ \Sigma_i\ A_i(C_i - C_{av})^2$
DR = density ratio ρ_j/ρ_∞
f = mixture fraction
H = duct height
h = enthalpy
J = momentum-flux ratio $(\rho_j V_j^2)/(\rho_\infty U_\infty^2)$, Eq. (1)
k_∞ = turbulent kinetic energy of mainstream
l/d = orifice thickness to diameter ratio
MR = mass-flow ratio m_j/m_∞
m_j = mass-flow of jets
m_∞ = mass-flow of mainstream
P_t = total pressure at plenum entrance
p = static pressure
p_{exit} = static pressure at combustor exit
p_{jet} = static pressure of jet
p_{s_1} = static pressure upstream of quick-mix orifices
p_∞ = static pressure of mainstream
T = temperature
T_{jet} = temperature of jet
T_∞ = temperature of mainstream
U_∞ = mainstream flow velocity
V_j = jet velocity
x = axial coordinate, 0 at leading edge of the orifice
x/H = axial distance-to-duct height ratio
y = vertical coordinate
z = lateral coordinate
ε_∞ = turbulent energy dissipation of mainstream
ρ_j = density of jet
ρ_∞ = density of mainstream
ϕ_{lb} = lean-burn equivalence ratio
ϕ_{rb} = rich-burn equivalence ratio

Presented as Paper 96-2762 at the AIAA/ASME/SAE/ASEE 32nd Joint Propulsion Conference, Lake Buena Vista, FL, July 1–3, 1996; received April 25, 1997; revision received May 25, 1998; accepted for publication July 26, 1998.

*Senior Engineer. Member AIAA.
†Vice President/Engineering. Member AIAA.
‡Research Scientist, Combustion Technology Group. Member AIAA.
§Senior Research Engineer, Turbomachinery and Propulsion Systems Division. Associate Fellow AIAA.

Introduction

THE mixing of jets with mainstream flow is very significant in many gas-turbine combustor applications. In conventional combustor design, air is injected through primary and dilution orifices to mix with hot gas effluent. The design of the orifices is important in combustor performance and durability, i.e., exit temperature pattern factor, exit radial temperature profile, combustion efficiency, emissions, linear hot streaks, etc. Many recent studies of confined jet mixing have been conducted on combustor components for advanced gas-turbine engines. NASA-supported studies are summarized in Refs. 1 and 2 for cylindrical and rectangular ducts, respectively. Previous studies, with smaller orifices in rectangular, cylindrical, and annular ducts, are summarized in Ref. 3. These summaries all contain rather substantial reference listings, including previous work of the authors and other researchers. Therefore, only those references that postdate these summaries, or from which material is specifically cited, are included herein. In all of these summaries the importance of the momentum-flux ratio and the spacing between adjacent orfices is delineated.

Recent jet mixing has drawn a lot of attention regarding low-emission combustor design, particularly the rich burn/quick mix/lean burn (RQL)[4] combustor design. The RQL combustor requires a large amount of bypass air (typically a jet-to-mainstream mass-flow ratio of 3), to be efficiently mixed with rich-burn effluent, so that NO_x emissions are kept to a minimum.[5]

Computational fluid dynamics (CFD) analysis is typically used to help design the orifice pattern for effective mixing. To conserve computer resources, CFD analysis is usually performed on the interior of the combustor; the inlet boundary conditions for the airjets are specified by the designer. The jets are typically input with uniform velocity and turbulence levels, and the flow direction is determined by one-dimensional annulus models. Usually, an effective orifice flow area is modeled, corresponding to the geometric area multiplied by an assumed discharge coefficient. Other research[6–10] has shown that there is a coupling between the annulus airflow and combustor interior flow. The prediction of jet penetration and mixing is strongly affected by including the annulus flow in the CFD analysis.

This paper studies mass-flow ratios typical of an RQL combustor. Instead of annulus flow, the airjets are fed by a plenum as a first step in understanding the coupling between jet and mainstream. A baseline plenum case is discussed first, and the nonuniformity of the jet exiting the orifice is presented. The CFD analysis is then verified by comparing isothermal numerical predictions with experimental measurements. Next, three cases of the combustor interior are analyzed to try to identify ways to specify jet boundary conditions that capture the flow coupling effects. And last, a thin-walled liner case is compared with a thick-walled liner case to assess the differences in flow coupling.

Details of Numerical Calculations

The focus of this study was to analyze the flow-coupling effects that can occur in jet-in-crossflow geometries. The baseline configuration, shown in Fig. 1, can be described as having an annular quick-mix zone with orifices located on both the inner- an outer-diameter liner. The orifices are fed by plenum chambers. The orifice thickness-to-diameter ratio, l/d = 0.3, represented a thick-walled combustor. The inner radius of the quick-mix zone annulus measured 38.96 cm and the outer radius measured 44.04 cm. The height of the quick-mix zone was 5.08 cm. The axial length of the calculation extended 15.2 cm from the leading edge of the orifice (x/H = 3.0). The walls, i.e., thickness of the orifices, were modeled as being 0.64 cm thick. Each orifice was fed by a plenum that was 6.5 cm in length, 7.6 cm in height, and 3.75 deg in width. The orifices were slots with semicircular ends and had 2:1 length-to-width aspect ratios. For the baseline thick-orifice case, the ratio of the jet geometric area to the mainstream cross-sectional area, A_j/A_∞, was 0.47. The i.d. and o.d. orifices were thus 1.35 cm × 0.67 cm each. (This was also the size for method 3 and the thin-orifice case discussed next.)

To enhance the computational efficiency of the numerical calculations, only one set of orifices (top and bottom) were modeled. The orifices were located on the i.d. and o.d. in the same axial plane, and inline in the transverse direction. For the cases presented here, there would be 96 opposed jet orifice pairs around the combustor circumference. The transverse calculation domain extended from midplane to midplane across the jets' centerline. Periodic boundary conditions were assumed on the transverse boundaries.

For the combustor-only calculations, only the quick-mix zone was used. The quick-mix orifices were modeled as inlets with a uniform velocity profile. The velocity magnitude was determined via three different methods that are shown in Fig. 2. The first method used the velocity calculated from the plenum to mixer exit pressure drop. The second method determined the pressure drop by using the total pressure in the plenum and the average static pressure across the quick-mix zone. The third method calculated a velocity based on the mass-flow through the geometric area of the orifice (C_d = 1). The jet velocities for these methods were calculated to be 155, 135, and 92 m/s, respectively. The mass flow through the jets was the same for all cases; hence, the area of the orifices was inversely proportional to the jet velocity. The ratio of the jet area for methods 1 and 2 to that for method 3 would be equal to the discharge coefficient, C_d, which is shown in Fig. 2. For the combustor-only calculations, the orifice sizes for methods 1, 2, and 3 were 1.05 × 0.52, 1.11 × 0.56, and 1.35 × 0.67 cm, respectively. The momentum-flux ratio, J, for each of the three cases is also given in Fig. 2, where

$$J = (DR)\left(\frac{V_j}{U_\infty}\right)^2 = \frac{(MR)^2}{(DR)(C_d)^2[(A_j/A_\infty)^2]} \tag{1}$$

Note that the number of orifices in the domain that is modeled is important; particularly for annular opposed jet configurations, i.e., MR results from flow through an orifice pair, and so A_j/A_∞ is the area ratio for the sum of both an i.d. and an o.d. orifice. Note also that for the calculations with a plenum chamber, a discharge coefficient must be assumed to determine a momentum-flux ratio. From previous experience, and the work reported in Ref. 11, it seems reasonable to assume C_d = 0.7 for the baseline case, thus giving J = 29, which is within

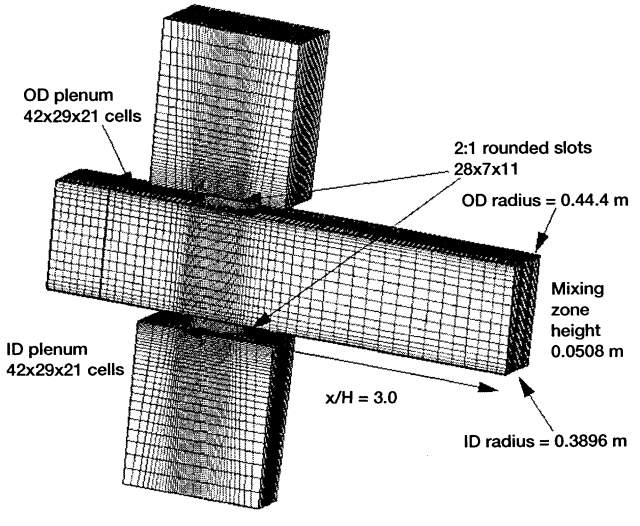

Fig. 1 Baseline annular geometry and grid.

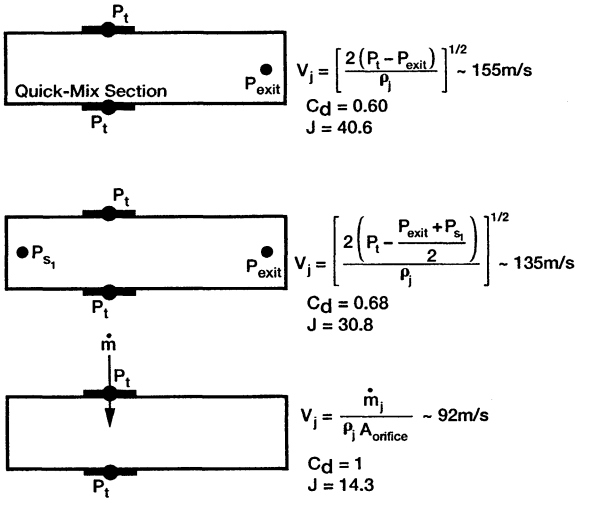

Fig. 2 Three methods used to determine jet velocity for combustor-only calculations.

the range of momentum-flux ratios for the combustor-only calculations.

To assess the effects of orifice thickness, a thin-walled geometry was also analyzed. The thin-walled case was identical to the baseline case, except for the orifice thickness. The wall thickness was reduced to 0.0889 cm for the thin-walled geometry.

The flow conditions of the mainstream and the jets were 1) mainstream: U_∞ = 43.5 m/s, T_∞ = 2035 K, p_∞ = 972 kPa, k_∞ = 118.0 m^2/s^2, and $\varepsilon_\infty = 5.4 \times 10^4$ m^2/s^3; and 2) jets: p_{jet} = 1030 kPa, and T_{jet} = 777 K, and MR = 3.20, DR = 3.20, ϕ_{rb} = 2.0, and ϕ_{lb} = 0.425.

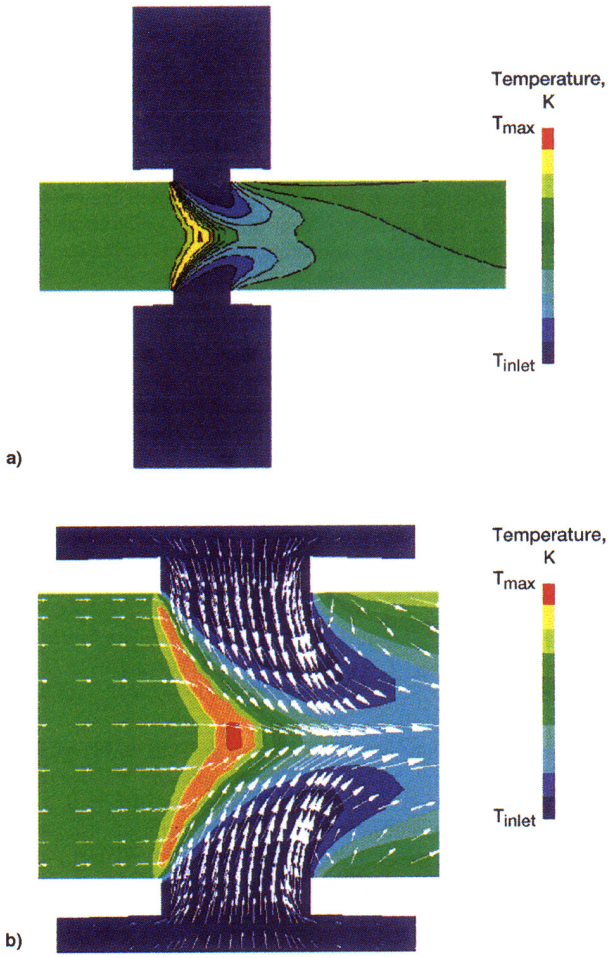

Fig. 3 Temperature contours for baseline plenum-fed geometry: a) center domain and b) closeup of jet (injection region).

Numerics and Models

The approach in this study was to perform three-dimensional numerical calculations on generic combustor geometries with and without the addition of plenum chambers. A code named CFD–ACE was used to perform all of the computations. The following conservation equations were solved: u momentum, v momentum, w momentum, mass (pressure correction), turbulent kinetic energy (k), turbulent energy dissipation (ε), and mixture fraction (f). The convective fluxes were calculated using upwind differencing, and the diffusive fluxes were calculated using central differencing. The standard k-ε turbulence model was employed and conventional wall functions were used. The walls were assumed to be adiabatic. The turbulent Schmidt and Prandtl numbers were set to be 0.5. A fast chemistry (instantaneous) model was assumed. Equilibrium products were also assumed. The inlet to the rich-burn section was assumed to be the equilibrium products of a fully burned 1.8 equivalence ratio. The fuel used was $C_{10}H_{19}$, representative of Jet A fuel.

Grids

The computational mesh was created using CFD–GEOM, an interactive three-dimensional geometry modeling and mesh generation software. The baseline case consisted of approximately 86,500 cells. The grid shown in Fig. 1 was created with five domains. Each plenum was modeled as a domain as well as each orifice. The quick-mix zone was also specified as a domain and was composed of 28,329 cells, 71 cells in the axial direction (x), 19 cells in the vertical direction (y), and 21 cells in the transverse direction (z). The plenum grid was distributed as 42 × 29 × 21 cells (x, y, and z directions). The 2:1 slots were composed of 28 × 11 uniformly distributed cells, with seven cells in the vertical direction to represent the combustor wall thickness (0.64 cm). The grid upstream and downstream of the slots was expanded/contracted so that each cell adjacent to the slot matched the cell size in the interior of the slot. The cells in the vertical direction were compressed in the wall regions to more accurately capture wall effects.

For the combustor-only case, a single domain mesh consisting solely of the quick-mix section was used. Finally, the thin-walled case was the same as the baseline case, except the thickness of the orifices was reduced.

Convergence

All error residuals were reduced at least six orders of magnitude, and continuity was conserved in each axial plane to the fifth decimal. A converged solution required approximately

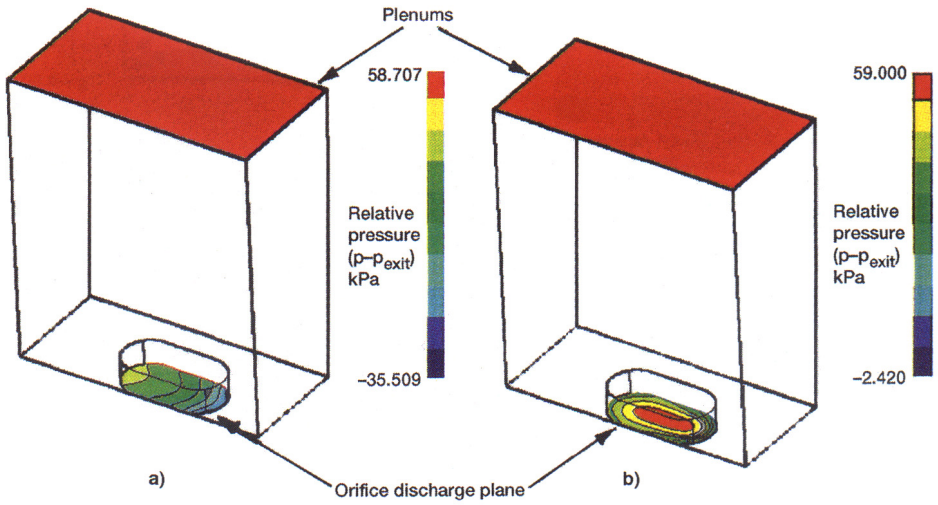

Fig. 4 Pressure distribution across the orifice exit plane: a) static and b) total pressures.

5–7 CPU hours on a IBM RS6000 Model 560 computer. Although the cases reported in this paper were performed using the IBM RS6000, additional cases were run using the NAS C-90 computer.

Results and Discussion

Baseline Plenum-Fed Case

Figure 3 shows the temperature contours for the baseline plenum-fed case. The temperature contours are plotted in a vertical–axial plane through the orifice centerline. The jets show near-optimum jet penetration, penetrating to approximately one-fourth duct height. There is a slight difference in penetration between the o.d. and i.d. jets; this difference is caused by geometric differences. The coupling causes a nonuniformity of the jet flowfield as it exits the orifice. By examining the velocity vectors and profile at the orifice exit (Fig. 3b), the jet velocity nonuniformity in the jet flowfield can be seen. Because the *l/d* is larger than for a conventional combustor, it is not surprising that the jet velocity is essentially normal to the crossflow. A low normal velocity is seen at the leading edge of the orifice and a high normal velocity at the trailing edge is evident.

Similarly, the static and total pressure at the orifice discharge was also nonuniform, as seen in Fig. 4. There is a high total pressure core in the center of the orifice, but at the edges of the orifice there is a total pressure loss. The nonuniform static pressure is further illustrated in the axial static pressure plot presented in Fig. 5. The static pressure varied from 30 kPa above the combustor exit pressure to 15 kPa below the combustor exit pressure.

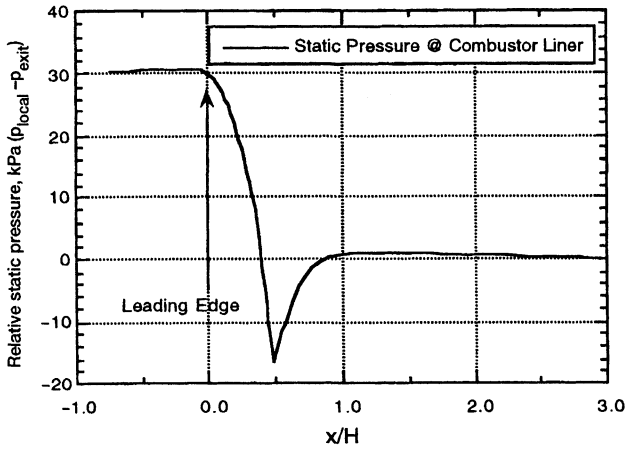

Fig. 5 Nonuniform static pressure at combustor liner (orifice extends from $0 < X/H < 0.5$).

Nonreacting Validation Case

To validate the plenum-fed baseline case, it was decided to perform a thick-orifice isothermal calculator case for which jet mixing data existed. The case selected is described next, with a comparison between numerical predications and experimental measurements.

Geometry

For this case, the geometry consisted of a cylindrical mixing zone with eight round holes uniformly spaced on the can circumference. Figure 6 shows a schematic of the test geometry [United Technologies Research Center (UTRC) Cylindrical Test Rig]. The diameter of each round hole was 1.78 cm (0.7 in.) and the i.d. of the can was 9.84 cm (3.88 in.). The thickness of each round hole was 3.97 cm (1.56 in.). The plenum was approximately 25.4 cm (10 in.) in diameter and 52.9 cm (6 in.) in length. The mainstream flow entered from an inlet section 30.48 cm long and 7.9 cm in diameter. The inlet section had a divergence angle of 2 deg with an initial diameter of 7.9 cm that diverges to the mixing section diameter of 9.84 cm. The orifices are located 5.08 cm downstream of the bulkhead that connects the mainstream inlet feed into the quick-mix region.

The computational grid is shown in Fig. 7. To enhance the computational efficiency of the numerical calculations, only one orifice was modeled (45-deg sector) and periodic boundaries were assumed. The grid was separated into three distinct blocks. The first block represented the quick-mix zone, consisting of 78 cells in the axial direction (x), 19 cells in the vertical direction (y), and 29 cells in the transverse (z) direction. The second block was the plenum; it was composed of $11 \times 14 \times 11$ cells (x, y, and z). The third block represented the orifice, composed of 29×29 uniformly distributed cells. The orifice was modeled with 14 cells in the vertical direction to represent the thickness of the combustor wall. In the quick-mix section, the grid upstream and downstream of the orifice region was expanded/contracted so that each cell adjacent to the orifice region matched the cell size in the slot region. The cells in the vertical direction were compressed in the vicinity of the wall to more accurately capture wall effects.

Flow Conditions

The flow conditions of the mainstream and jets were specified to be 1) mainstream: $U_\infty = 4.64$ m/s, $T_\infty = 291.67$ K, $p_\infty = 101.3$ kPa, $k_\infty = 2.90 \times 10^{-2}$ m^2/s^2, and $\varepsilon_\infty = 3.21 \times 10^{-1}$ m^2/s^3; and 2) jets: $p_{jet} = 106.17$ kPa and $T_{jet} = 291.67$ K. The

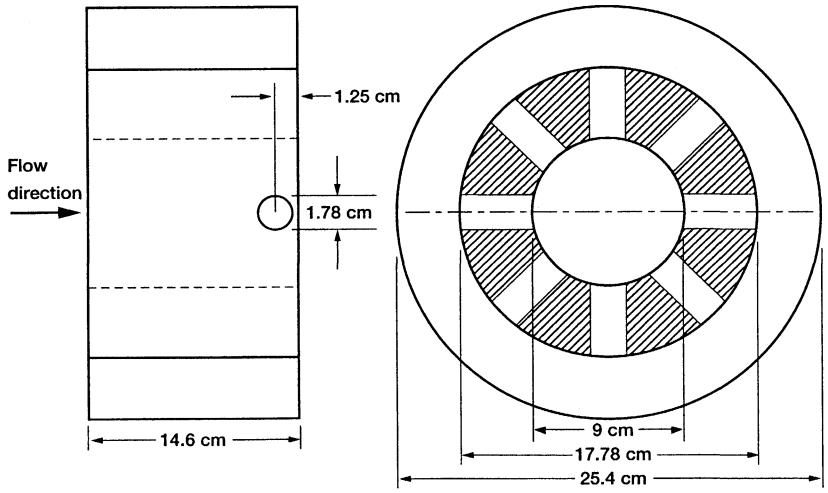

Fig. 6 Schematic of UTRC Cylindrical Test Rig.

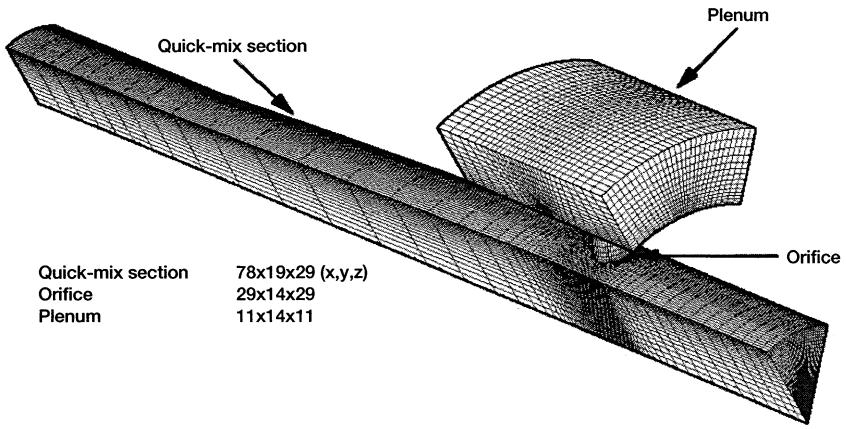

Fig. 7 Computational mesh for UTRC cylindrical geometry.

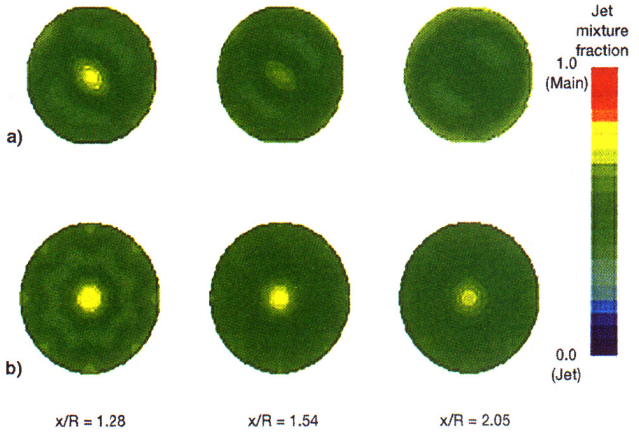

Fig. 8 Comparison between CFD-ACE calculations and UTRC experimental measurements.

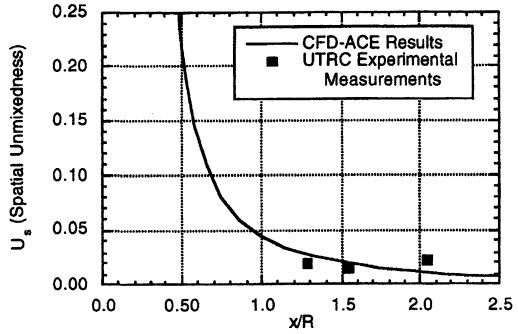

Fig. 9 Numerical and experimental comparison of spatial unmixedness.

mass-flow ratio for this case was specified to be 1.0 and corresponded to a momentum-flux ratio of 30.

Validation Case Results

The jet mixture fraction axial slice measurements and the comparable numerical results are shown in Fig. 8. Axial slices were extracted at x/R locations of 1.28, 1.54, and 2.05 downstream of the leading edge of the round hole. The same color bar was used for the calculated results and experimental measurements. The numerical results show very good agreement with the experimental results at all of the downstream stations. At the closest station (x/R = 1.28), the computational results capture the center mainstream core along with the slight bluish contour levels present at about midradius. Moving to the locations farther downstream, the numerical results show a slightly slower mixing rate than seen in the experimental results.

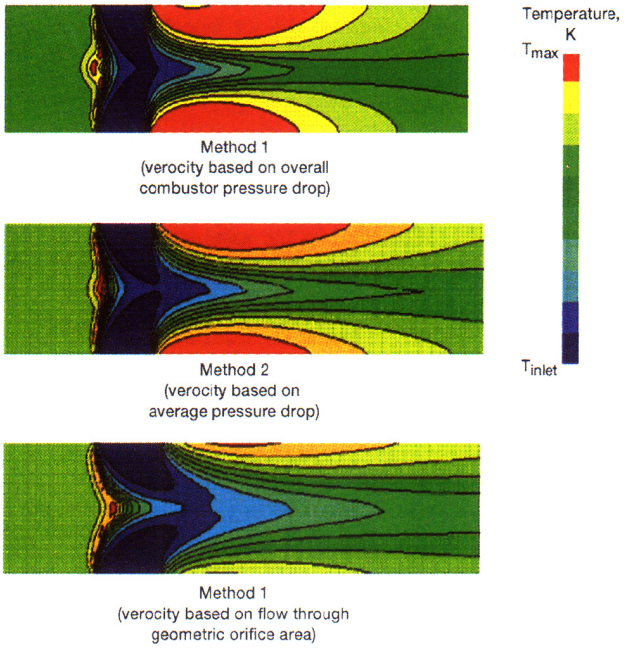

Fig. 10 Combustor-only analysis (compared with Fig. 3).

Figure 9 shows the spatial unmixedness curves for the CFD and experimental results. Planar unmixedness, U_s,[12] is a parameter that quantifies the unmixedness of a distribution and can be defined as

$$U_s = C_{var}/[C_{av}(1 - C_{av})] \tag{2}$$

where

$$C_{var} = \frac{1}{A_{tot}} \sum_{i=1}^{M} A_i(C_i - C_{av})^2$$

C_{av} = planar average concentration and C_i = local concentration. Good overall agreement can be seen. Thus, from an engineering viewpoint, the plenum-fed calculation seems to capture the overall characteristics of jets-in-confined-crossflow.

Combustor-Only Calculations

Figure 10 shows results of the combustor-only calculations for three specified uniform inlet velocities: 1) jet velocity corresponding to the overall pressure drop, 155 m/s; 2) jet velocity corresponding to the average pressure drop, 135 m/s; and 3) jet velocity corresponding to the mass-flow through the orifice geometric area, 92 m/s. Compared with the baseline calculation (Fig. 3), each combustor-only case predicted jet over-

penetration. The highest jet velocity produced the greatest amount of overpenetration, as evidenced by the mainstream flow being deflected to the outer wall. This is illustrated by the hotter temperatures near the i.d. and o.d. walls. The results of the lowest jet velocity (method 3) still predicted overpenetrating jets, but gave the closest overall agreement to the baseline case results. Note that the o.d. near-wall temperatures are hotter than the i.d. temperature for each case. This occurs because the orifice spacing is slightly greater for the o.d. wall, resulting in more mainstream flow passing between the jets.

Thus, it appears that there is no simple way to capture the flow coupling that occurs with plenum-fed flowfields. As discussed previously for the baseline plenum geometry, there exists nonuniformity in the jet flow at the discharge orifice plane. To use an inlet boundary condition for the orifice, one would have to devise a way to determine the velocity profile that correctly produces the flow nonuniformity at the orifice discharge. This includes correctly modeling the nonuniform velocity profile, turbulence quantities, and the flow angle. The determination of these factors creates potential problems because of their variation across the orifice cross-sectional area. If it was possible to ascertain an acceptable method of capturing the flow nonuniformity, there is no guarantee that this method would be generally applicable to a variety of different orifice shapes, momentum-flux ratios, and spacing. Therefore, from a design standpoint, it probably would be very difficult to accurately capture the jet coupling effect without the use of the plenums.

Effect of Wall Thickness

For completeness, analysis was performed on a thin-walled liner to assess the effect of wall thickness on the flow coupling. Figure 11 presents the temperature contour results of the thin-walled case. Compared with the thick-walled case (Fig. 3), the thin-walled geometry showed higher jet penetration and higher overall downstream mixing.

Based on the work performed by Lichtarowicz et al.,[11] it would be safe to assume that the thin-walled configuration (l/d = 0.04) would have a smaller discharge coefficient than the thick-walled (baseline) design (l/d = 0.3). The lower C_d in the thin-walled case would then result in an increased pressure drop across the orifice for the same mass-flow ratio. The total pressure variation for the two geometries is presented in Fig. 12. The pressure drop, plenum total pressure-combustor total pressure, for the thin-walled case is about 6.5%, whereas the thick-walled case has a pressure drop around 5.8%. Despite the variation in C_d, the normal velocity levels were essentially the same for both cases. The comparable velocity levels for

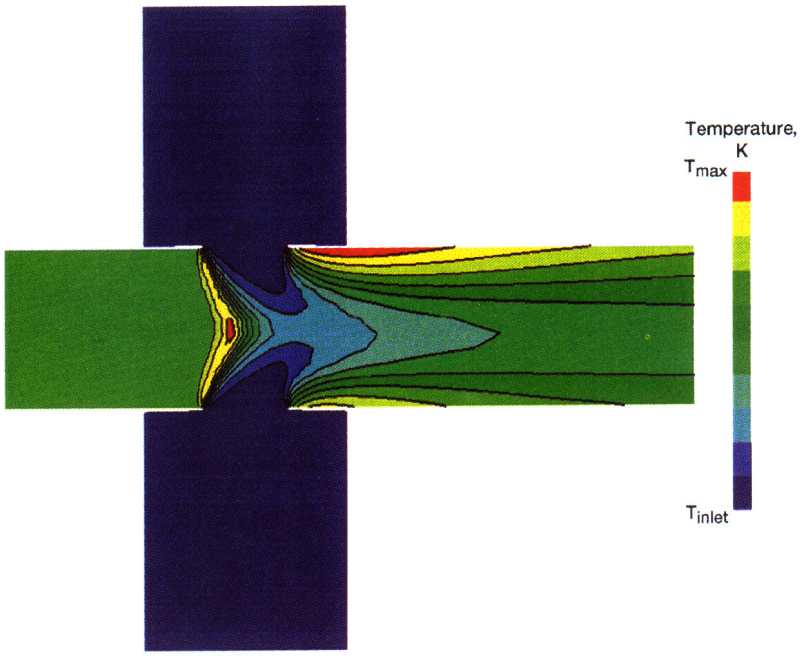

Fig. 11 Temperature contours for the thin-walled geometry (compare with Figs. 3 and 11).

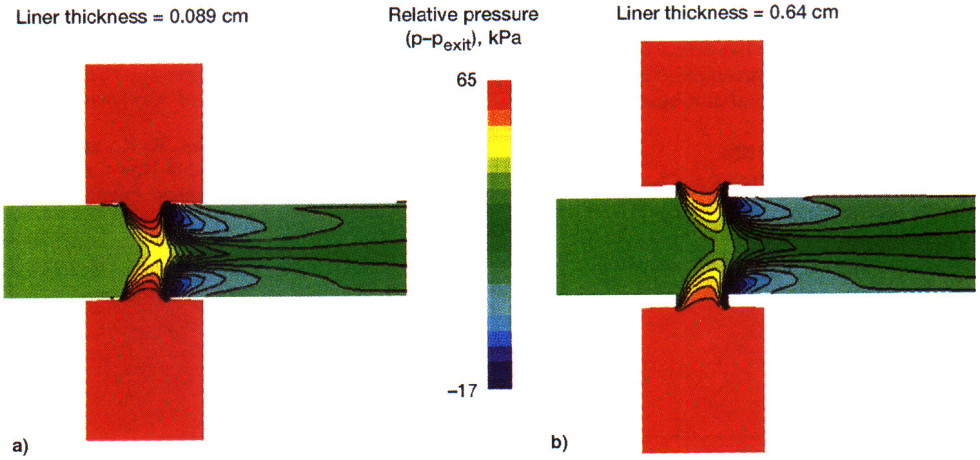

Fig. 12 Total pressure centerline slices for a) thin and b) thick-walled geometry.

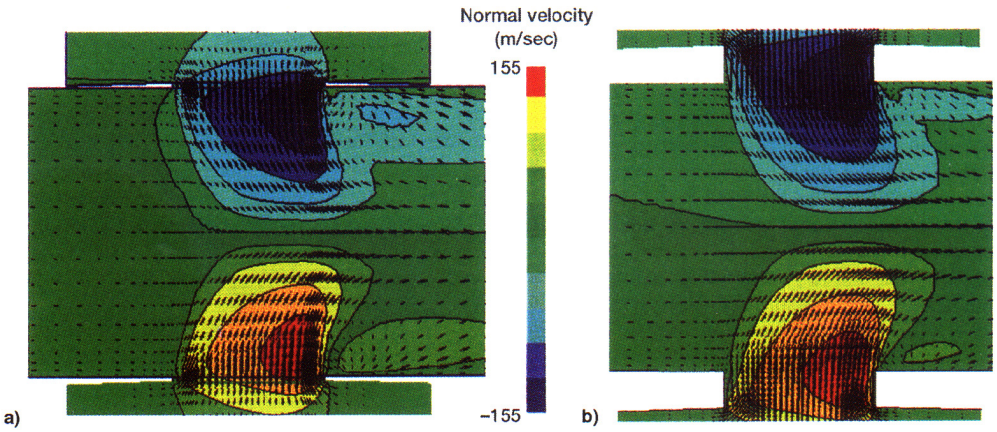

Fig. 13 Velocity profile comparison between a) thin-walled geometry and b) baseline plenum-fed thick-walled geometry.

both the thin- and thick-walled cases are shown in Fig. 13. The differences in the penetration levels for the thick- and thin-walled cases can be addressed by examining the velocity profiles. The velocity flowfield for both cases exhibit similar characteristics, but one significant difference seen is that the velocity profiles for the thin-walled case are pushed farther into the mainstream flow. This inboard translation of the velocity profiles results in more jet penetration into the quick-mix zone with the thin-walled case. Thus, the increased jet penetration can be directly attributed to the smaller discharge coefficient and, subsequently, the higher pressure drop evident in the thin-walled case. The importance of modeling the flow through the orifice is thereby shown.

Conclusions

CFD analyses were performed on airjets injected to rich-burn effluent flowing in an annulus. Jet-to-mainstream mass-flow ratios (~3) typical of RQL combustors were analyzed. Two types of calculations were performed: 1) only the combustor was modeled, with the jet flow specified at the orifice discharge plane; and 2) the jet plenum and orifice were included in the calculation domain. The following are results from the analysis.

1) There exists a strong coupling between the jet flow and mainstream flow evidenced by the large-velocity profile at the orifice exit.

2) This coupling could not be easily captured by specifying commonly used uniform jet velocity boundary conditions for combustor-only CFD calculations.

3) The only way to accurately predict jet-in-crossflow flowfields is to include both the interior and exterior (plenums) flowfields in the CFD analysis. To do this, more computational expense is required, but it is possible with modern workstations, many-to-one grid topologies, multiblock gridding techniques, and/or parallel processing.

4) CFD analysis was able to capture the effect of liner thickness on jet penetration and mixing, provided the calculation domain included the external and internal combustor geometry.

Acknowledgments

The CFD work was supported by NASA Contract NAS3-25967, and NAS computer time was provided by NASA Lewis Research Center. The authors would like to thank the CFDRC software development and support staff for implementing improvements to the software. The experiment was performed at United Technologies Research Center with support from NASA Contract NAS 3-25954, Task Order #12.

References

[1]Holdeman, J. D., Liscinsky, D. S., Oechsle, V. L., Samuelsen, G. S., and Smith, C. E., "Mixing of Multiple Jets with a Confined Subsonic Crossflow: Part I—Cylindrical Ducts," *Journal of Engineering for Gas Turbines and Power*, Vol. 119, Oct. 1997; also American Society of Mechanical Engineers, Paper 96-GT-482, 1996, and NASA TM-107185.

[2]Holdeman, J. D., Liscinsky, D. S., and Bain, D. B., "Mixing of Multiple Jets with a Confined Crossflow: Part II—Opposed Rows of Orifices in Rectangular Ducts," American Society of Mechanical Engineers, Paper 97-GT-439, June 1997; also NASA TM-107461.

[3]Holdeman, J. D., "Mixing of Multiple Jets with a Subsconic Crossflow," *Progress in Energy and Combustion Science*, Vol. 19, 1993, pp. 31–70; also NASA TM-104412.

[4]Shaw, R. J., "Engine Technology Challenges for a 21st Century High Speed Civil Transport," ISABE 10th International Symposium on Air Breathing Engines, Sept. 1991; also NASA TM-104363.

[5]Mosier, S. A., and Pierce, R. M., "Advanced Combustion Systems for Stationary Gas Turbine Engines," PB80-175599/FR11405-Vol-1/EPA 600/7-80-17A-Vol-1, 1980.

[6]Carrotte, J. F., and Stevens, S. J., "The Influence of Dilution Hole Geometry on Jet Mixing," *Journal of Engineering for Gas Turbines and Power*, Vol. 112, No. 1, 1990, pp. 73–75; also American Society of Mechanical Engineers, Paper 89-GT-292, 1989.

[7]Stevens, S. J., and Carrotte, J. F., "Experimental Studies of Combustor Aerodynamics, Part I: Mean Flowfields," *Journal of Propulsion and Power*, Vol. 6, No. 3, 1990, pp. 297–304; also "The Influence of Dilution Hole Aerodynamics on the Temperature Distribution in a Combustor Dilution Zone," AIAA Paper 87-1827, 1987.

[8]Stevens, S. J., and Carrotte, J. F., "Experimental Studies of Combustor Dilution Zone Aerodynamics, Part II: Jet Development," *Journal of Propulsion and Power*, Vol. 6, No. 4, 1990, pp. 503–511; also AIAA Paper 88-3274, 1988.

[9]McGuirk, J. J., and Baker, S. J., "Multi-Jet Annulus/Core-Flow Mixing-Experiments and Calculations," American Society of Mechanical Engineers, Paper 92-GT-111, 1992.

[10]McGuirk, J. J., and Spencer, A., "CFD Modeling of Annulus/Port Flows," American Society of Mechanical Engineers, Paper 93-GT-185, 1993.

[11]Lichtarowicz, S., Duggins, R. K., and Markland, E., "Discharge Coefficients for Incompressible Non-Cavitating Flow Through Long Orifices," *Journal of Mechanical Engineering Science*, Vol. 7, No. 2, 1965, pp. 210–219.

[12]Danckwertz, P. V., "The Definition and Measurements of Some Characteristics of Mixtures," *Appl. Sci. Res.*, Sec. A, Vol. 3, 1952, pp. 279–296.

Color reproductions courtesy of NASA Lewis Research Center.